RESEARCH ARTICLE

Protective Efficacy of Inactivated Vaccine against SARS-CoV-2 Infection in Mice and Non-Human Primates

Yan-Feng Yao[1] · Ze-Jun Wang[2] · Ren-Di Jiang[1,3] · Xue Hu[1] · Hua-Jun Zhang[1] · Yi-Wu Zhou[4] ·
Ge Gao[1] · Ying Chen[1,3] · Yun Peng[1] · Mei-Qin Liu[1,3] · Ya-Nan Zhang[1,3] · Juan Min[1] · Jia Lu[2] · Xiao-Xiao Gao[1] ·
Jing Guo[2] · Cheng Peng[1] · Xu-Rui Shen[1,3] · Qian Li[1,3] · Kai Zhao[1,3] · Lian Yang[5] · Xin Wan[2] · Bo Zhang[1] ·
Wen-Hui Wang[2] · Jia Wu[1] · Peng Zhou[1] · Xing-Lou Yang[1] · Shuo Shen[2] · Chao Shan[1] · Zhi-Ming Yuan[1] ·
Zheng-Li Shi[1]

Abstract

The ongoing coronavirus disease 2019 (COVID-19) pandemic caused more than 96 million infections and over 2 million deaths worldwide so far. However, there is no approved vaccine available for severe acute respiratory syndrome coronavirus 2 (SARS-CoV-2), the disease causative agent. Vaccine is the most effective approach to eradicate a pathogen. The tests of safety and efficacy in animals are pivotal for developing a vaccine and before the vaccine is applied to human populations. Here we evaluated the safety, immunogenicity, and efficacy of an inactivated vaccine based on the whole viral particles in human ACE2 transgenic mouse and in non-human primates. Our data showed that the inactivated vaccine successfully induced SARS-CoV-2-specific neutralizing antibodies in mice and non-human primates, and subsequently provided partial (in low dose) or full (in high dose) protection of challenge in the tested animals. In addition, passive serum transferred from vaccine-immunized mice could also provide full protection from SARS-CoV-2 infection in mice. These results warranted positive outcomes in future clinical trials in humans.

Keywords Severe acute respiratory syndrome coronavirus 2 (SARS-CoV-2) · Coronavirus disease 2019 (COVID-19) · Inactivated vaccine · Transgenic mouse · Non-human primate

---

Yan-Feng Yao, Ze-Jun Wang, Ren-Di Jiang, Xue Hu, and Hua-Jun Zhang contributed equally to this work.

✉ Zheng-Li Shi
zlshi@wh.iov.cn

✉ Zhi-Ming Yuan
yzm@wh.iov.cn

✉ Chao Shan
shanchao@wh.iov.cn

✉ Shuo Shen
shenshuo1@sinopharm.com

✉ Xing-Lou Yang
yangxl@wh.iov.cn

[1] Center for Biosafety Mega-Science, Wuhan Institute of Virology, Chinese Academy of Sciences, Wuhan 430071, China

Introduction

The ongoing coronavirus disease 2019 (COVID-19) has caused public health crisis to people all of the world, and leads to over 96 million of infections and 2 million of death

[2] Wuhan Institute of Biological Products Co. Ltd, Jiangxia District, Wuhan 430024, China

[3] University of Chinese Academy of Sciences, Beijing 100049, China

[4] Department of Forensic Medicine, Tongji Medical College of Huazhong University of Science and Technology, Wuhan 430074, China

[5] Department of Radiology, Union Hospital, Tongji Medical College, Huazhong University of Science and Technology, Wuhan 430074, China

worldwide (WHO 2020a). Drugs and compounds, such as remdesivir, chloroquine diphosphate, and favipiravir have been proved to have high antiviral activity *in vitro*, but the outcomes of their clinical trials have been controversial, thus there is still no SARS-CoV-2 specific drugs so far (Wang M *et al.* 2020). Protective antibodies are good candidates for neutralizing virus infection and treating COVID-19 patients at early infection stage, but these treatments are at high cost (Baum *et al.* 2020; WHO 2020b). Thus, vaccination is still an ultimate measure to end this likely long-term pandemic (Kissler *et al.* 2020).

SARS-CoV-2, the etiologic agent responsible for the COVID-19, was a member of the *Cornaviridae* family, a single-stranded and positive-sense RNA virus. SARS-CoV-2 uses angiotensin-converting enzyme 2 (ACE2) as its binding receptor, and the spike protein is the main target for neutralizing antibodies (Coronaviridae Study Group of the International Committee on Taxonomy of 2020; Hoffmann *et al.* 2020; Zhou *et al.* 2020). Antigen selection and engineering, preclinical challenge studies, and immune correlates of protection are core issues for vaccine evaluation (Dagotto *et al.* 2020). Currently, multiple vaccine pipelines against SARS-CoV-2 are under development and clinical trials, such as nuclear acid-based, subunits containing viral epitopes, adenovirus-based vectors, and the whole inactivated virus (Corbett *et al.* 2020a, 2020b; Gao *et al.* 2020; Tostanoski *et al.* 2020; van Doremalen *et al.* 2020; Wang H *et al.* 2020; Wu *et al.* 2020; Xia *et al.* 2020; Yang *et al.* 2020; Yu *et al.* 2020).

Safety, immunogenicity, and protection efficacy are pivotal for developing a vaccine and need tests in animals before being applied to humans. Based on our long-term history and well-established technology for developing inactivated virus vaccines, we rapidly developed SARS-CoV-2 inactivated virus (IAV) as vaccine candidate using a viral strain that was isolated from the bronchoalveolar lavage fluid (BALF) sample collected from a patient with COVID-19 (Zhou *et al.* 2020). This vaccine has been proved safe and immunogenicity in 7 different animal species and in phase I and II clinical trials in Wuzhi County, China, since the 12th and 24th of April, 2020, respectively (Wang ZJ *et al.* 2020; Xia *et al.* 2020). The phase III clinical trial is undergoing in more than ten countries. Previously, we have established the human ACE2 transgenic (HFH4-hACE2) mouse infection model and non-primate Rhesus macaque infection model for SARS-CoV-2 (Jiang *et al.* 2020; Shan *et al.* 2020). Here we reported the safety, immunogenicity, and efficacy of the inactivated vaccine candidate in HFH4-hACE2 mice and rhesus macaque, before going for human clinical trials.

Materials and Methods

Virus, Cell, and Antibody

SARS-CoV-2 (IVCAS 6.7512) was isolated from a bronchoalveolar lavage fluid collected from a patient with viral pneumonia in December 2019 in Wuhan, China. The virus isolation was propagated in Vero E6 cells (ATCC® CRL-1586™) in DMEM supplemented with 10% fetal calf serum, 1 mmol/L L-glutamine, 100 international units (IU)/mL penicillin, and 100 μg/mL streptomycin and cultured at 37 °C in 5% CO_2. The virus was harvested on day 3 post infection. Virus titrations were performed by end-point titration in Vero E6 cells. Cells were inoculated with tenfold serial dilutions of cell supernatant. One hour after inoculation of cells, the inoculum was removed and replaced with 100 μL of DMEM supplemented with 2% fetal bovine serum. Three days after inoculation, the cytopathic effect was scored, and the $TCID_{50}$ was calculated. The anti-SARS-CoV-2 N protein antibody was made in house. And Cy3-conjugated goat-anti-rabbit IgG was purchased Abcam (Cambridge, UK).

Preparation of the Inactivated SARS-CoV-2 Vaccine

The inactivated vaccine was prepared as below and quality control methods were submitted for patent applications. Briefly, SARS-CoV-2 virus was used to infect Vero cells. The supernatant was harvested on day 3–4 days when cytopathic effect (CPE) was shown. Then β-propiolactone was added into the supernatant at 1:4000 (*v/v*) at 2 °C–8 °C for 48 h to inactivate virus, followed by cell debris clarification, ultrafiltration. After 2nd β-propiolactone-inactivation, gel-chromatography, ion-exchange chromatography, sterile filtration, the viral particles were formulated with buffer and aluminum hydroxide adjuvant and packaged with label. Inactivation was validated by passaging the treated samples 3 generations without appearance of CPE. The in-process quality controls were established and applied.

IAV Evaluation in hACE2 Mice

Six to eight weeks old HFH4-hACE2 mice (5/group) were used for the IAV immunogenicity and efficacy study (Menachery *et al.* 2016). The mice were immunized on day 0 and 14 with dose 5 μg or 10 μg of IAV by intraperitoneal route, aluminum hydroxide with PBS used in control group. Blood samples were collected at 0, 9, 14, 21, 28 days after vaccination by retro-orbit (RO) route. All the mice were challenged on the day 28 after primary

immunization with dose 10^5 TCID$_{50}$/mouse by intranasal route. The body weight of mice was monitored daily after challenge. All the mice were euthanized on day 5 post challenge and the lungs were used for viral load and pathological analysis.

Antibody Passive Transfer Study in hACE2 Mice

Six to eight weeks old HFH4-hACE2 mice (5/group) were used for the passive transfer study. Mice sera were collected from BALB/c immunized with 5 μg of IAV and pooled. Six to eight weeks old HFH4-hACE2 mice (5/group) were then intraperitoneally injected with 100 μL of pooled vaccinated neat or 1:3, 1:9, 1:27 diluted sera. The control groups were using uninfected healthy mice sera or PBS. Mice were intranasally infected with 10^5 TCID$_{50}$ of SARS-CoV-2 after RO bleeding at day 1 post infection. All the mice were euthanized on day 5 post challenge and the lungs were used for viral load and pathological analysis.

IAV Evaluation in Rhesus Macaques

Nine rhesus macaques (RM) (age 6–7 years, weight 6–10 kg) divided into 3 groups (sham vaccine (VC), high dose group (VH), and low dose group (VL)) and were inoculated with aluminum hydroxide adjuvant only, 25 μg IAV and 5 μg IAV on day 0 and 14. The blood was bled on day 0, 7, 14, and 21 days and sera were collected for neutralizing antibody test. The RMs were challenged on the day 28 after primary immunization with dose 10^6 TCID$_{50}$/monkey intratracheally. The RMs were observed daily, with detailed recording of clinical signs, symptoms, morbidity, and mortality, including the nature, onset, severity, and duration of all gross or visible changes. Swab samples of the oropharyngeal, nasal turbinate, and rectal regions were collected at 1–7, 9- and 13-days post challenge (d.p.c.). To confirm the pathogenesis and injury in the respiratory tract, one animal from each group was sacrificed at 4, 9, and 13 d.p.c., respectively. The trachea, right bronchus, left bronchus and all six lung lobes were collected on the day of euthanization for various pathological, virological, and immunological analysis.

Quantitative Reverse Transcription Polymerase Chain Reaction

Viral RNA in the samples was quantified by one-step real-time quantitative RT-PCR. The swab and blood samples were used to extract viral RNA by using the QIAamp Viral RNA Mini Kit (Qiagen, Hilden, Germany), according to the manufacturer's instructions. Tissues were homogenized in DMEM (1:10, *w/v*), clarified by low-speed centrifugation at 4500 $\times g$ for 30 min at 4 °C, and supernatant was immediately used for RNA extraction. RNA was eluted in 50 μL of elution buffer and used as the template for RT-PCR. The primers pairs were used following our previous study which is targeting *S* gene: RBD-qF1: 5′-CAATGGTTTAACAGGCACAGG-3′; RBD-qR1: 5′-CTCAAGTGTCTGTGGATCACG-3′. Two microliters of RNA were used to verify the RNA quantity by HiScript® II One Step qRT-PCR SYBR® Green Kit (Vazyme Biotech Co., Ltd, Nanjing, China) according to the manufacturer's instructions. The amplification was performed as followed: 50 °C for 3 min, 95 °C for 30 s followed by 40 cycles consisting of 95 °C for 10 s, 60 °C for 30 s, and a default melting curve step in an ABI stepone machine.

Quantitative of Total Specific Antibodies in Sera

The total specific antibodies were detected with ELISA. Purified inactivated virions were coated in 96-well plates with 100 ng/well at 4 °C overnight. The plates were blocked with 0.01 mol/L PBST-1% bovine serum albumin (BSA) at 37 °C for 1 h. Serum samples, in a tenfold or two-fold series of dilutions, were added per well and incubated for 1 h at 37 °C. Then diluted HRP-conjugated antibodies against IgG (Boster Biological Technology, Pleasanton, CA, USA) of different hosts were added and incubated for 1 h. Between each step, the wells were washed 5 times with PBST. Following the addition of substrates for 30 min, the reaction stop solution was added, OD450 and OD630 values were read, and values higher than cut-off value of 0.15 was considered as positive.

Histopathology and Immunohistochemistry

Animal necropsies were performed according to a standard protocol. Tissues for histological examination were stored in 10% neutral-buffered formalin for 7 days, paraffin-embedded, sectioned, and stained with hematoxylin and eosin (H&E) prior to examination by light microscopy. To examine the SARS-CoV-2 antigen, paraffin dehydrated tissue sections were placed in antigen repair buffer for antigen retrieval in a microwave oven. The tissue was blocked with 5% BSA at room temperature for 1 h, following with house-made primary antibody at 1:500 (rabbit anti-SARS-CoV-2 N protein polyclonal antibody). After washed by PBS, the slices were slightly dried and covered with Cy3-conjugated goat-anti-rabbit IgG (Abcam) at 1:200 dilution. The slides were stained with DAPI (5 μg/mL) after washing by PBS. The image was collected by Pannoramic MIDI system (3DHISTECH, Budapest, Hungary).

Neutralizing Antibody Titer

The virus neutralization test was performed in a 12-well plate. The serum samples from mice and RMs were heat-inactivated at 56 °C for 30 min. The serum samples were diluted to 1:50, 1:150, 1:450, 1:1350, 1:4050, and 1:12150, and then an equal volume of virus stock was added and incubated at 37 °C in a 5% CO_2 incubator. After 1 h incubation, 100 μL mixtures were inoculated onto monolayer Vero cells in a 12-well plate for 1 h with shaking every 15 min. The inocula was removed and cells were incubated with DMEM supplemented with 2% FBS containing 0.9% methylcellulose 3 days before fix. The cells were fixed with 4% formaldehyde after 3 days inoculation for 30 min. Then the solution was removed and washed by tap water, followed by crystal violet staining. The plaques were counted for calculating the titer.

Results

IAV Protects HFH4-hACE2 Mice from SARS-CoV-2 Infection

To evaluate the immunogenicity of IAV for SARS-CoV-2, we intraperitoneally immunized 6–8 weeks old female HFH4-hACE2 mice with either low doses (5 μg), high dose (10 μg) of IAV, or sham vaccine, each comprising five mice. Mice were injected with IAV with D0/D14 immunization programs and then challenged with 10^5 $TCID_{50}$ per each SARS-CoV-2 virus. Body weight was monitored daily. Blood samples were collected at 0, 9, 14, 21, and 28 days after the injections, and also collected at each day after viral infection. All mice were sacrificed 5 days after viral infection and tested for lung viral load and pathology changes (Fig. 1A). Virion specific IgG antibodies were tested in ELISA and neutralizing antibody titers were determined by plaque reduction neutralization test (PRNT). There was a robust increase of virion IgG responses from day 7 to day 21 in vaccinated groups, but no difference between the two dose groups (Fig. 1B). The similar pattern was observed in neutralizing antibody production, although the titer appears higher in high dose group at 14 days after vaccination (Fig. 1C). We then assessed the protective efficacy in vaccinated or sham vaccine mice. Upon infection, there was no obvious weight loss changes among the three groups (Fig. 1D). However, the amount of viral RNA copies in lung was undetectable in high dose group and significantly decreased in low dose group, in contrast to a high viral load in mock group (Fig. 1E). To examine the disease severity and viral protein of SARS-CoV-2, the lungs in different groups were analyzed with H&E or

immunofluorescence assay (IFA) anti-SARS-CoV-2 nucleocapsid protein (N) antibody staining. Moderate pathological changes were observed in mock group, including the inflammatory infiltration at peri-bronchiolar and peri-vascular, alveolar wall thickening, and fibrin exudation (Fig. 2). In contrast, the pathological changes were almost absent in lung of high dose group, and much milder in low dose group. Collectively, the average pathology score was lower in the vaccinated mice than the mock mice (Supplementary Fig. S1A). The IFA results confirmed that viral antigen was mainly present in mock group but absent or decreased in vaccinated mice (Fig. 2).

Immune Serum upon Vaccination Protected Mice from SARS-CoV-2 Infection

To determine the protective efficacy of antibodies induced through vaccination, passive transfer test was performed in this study. Mouse sera were collected from BALB/c immunized with 5 μg of IAV and pooled. Five male six-eight weeks old HFH4-hACE2 mice in each group were then intraperitoneally injected with 100 μL of pooled vaccinated neat or 1:3, 1:9, and 1:27 diluted mouse sera with control groups using uninfected healthy mouse sera or PBS. On day 1 after injection, mice were intranasally infected with 10^5 $TCID_{50}$ of SARS-CoV-2 after retro-orbit (RO) bleeding (Fig. 3A). The data demonstrated that either virion-based IgG antibodies or neutralizing antibodies were stably persistent at least 5 days in passive transferred mice (Fig. 3B, 3C). While there was no obvious body weight difference among all groups, viral RNA load in lung was undetectable in neat and 1:3 diluted groups (Fig. 3D, 3E). While the amount of viral RNA levels in 1:9 or 1:27 groups was comparable to negative sera or PBS groups. At day 5 post infection, the mice were necropsy, and lungs were sectioned and stained with (H&E) and anti-SARS-CoV-2 N antibody. Lungs in neat and 1:3 dilution group appears normal except few exude of fibrin in some alveolar spaces in 1:3 dilution group. In other four groups, lungs show similar pathology changes with moderate alveolar wall thickening, mild peri-bronchial and peri-vascular infiltration and alveolar exudation of fibrin (Fig. 4, Supplementary Fig. S1B). Consistent to pathological observations, viral antigen was not found in neat or 1:3 dilution group either (Fig. 4).

IAV Protect the Rhesus Monkeys from the Infection of SARS-CoV-2

To further evaluate the immunogenicity of IAV for SARS-CoV-2 in nonhuman primate, we launched a small-scale vaccine protection experiment in RMs. RMs were immunized by the intramuscular route with SARS-CoV-2 IAV at

Fig. 1 Inactivated SARS-CoV-2 vaccine protects mice from SARS-CoV-2 infection. Six to eight weeks old HFH4-hACE2 mice were intraperitoneally injected with two different doses (5 μg or 10 μg) in D0/D14 immunization programs. Mouse sera was collected at 0, 9, 14, 21, 28 days post initial vaccination, and mice were challenged with 10^5 $TCID_{50}$ SARS-CoV-2 and followed with 5 days monitoring period. The experiment scheme was shown (**A**). Humoral antibody response in vaccinated mouse sera was detected by virion-based IgG ELISA (**B**) and $PRNT_{50}$ (**C**). Mouse body weight was recorded for 5 days (**D**), and lung viral load was determined by using RT-qPCR. Error bars indicate the standard error. Dotted line represents the limit of detection (L.O.D).
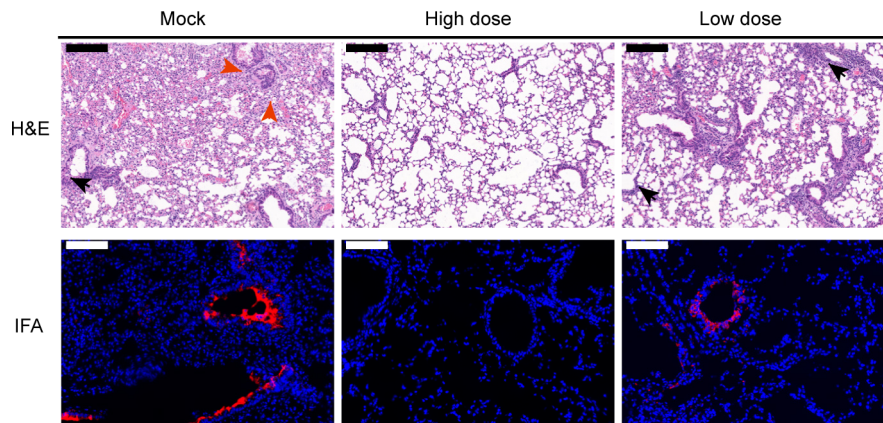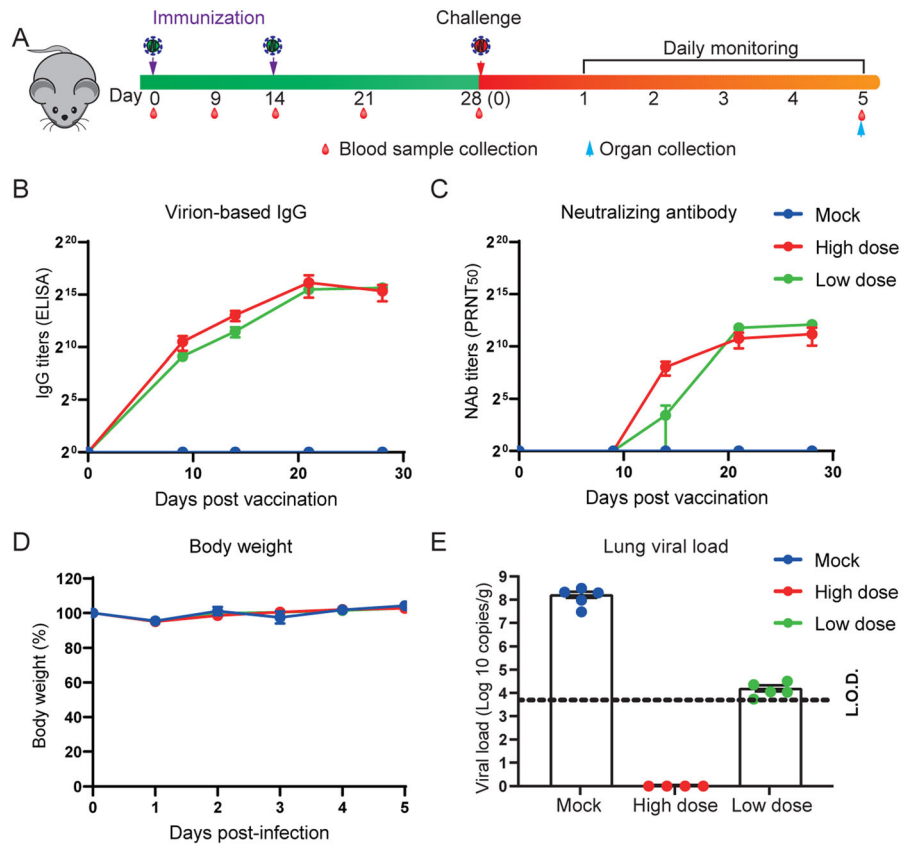

Fig. 2 Pathological changes in vaccinated mouse lung after challenge. Mock lung shows massive alveolar disappear, peri-bronchial, peri-vascular infiltration (black arrow), and exudation of fibrin (red arrow). There was no obvious lung damage in high dose vaccinated animals. In low dose vaccinated mouse lung, mild peri-bronchial infiltration was observed (black arrow). In IFA images, viral antigen was detected by anti-SARS-CoV-2-RBD polyclonal antibody (red). Images were collected by using Pannoramic MIDI system. Black scale bars indicate 200 μm and white scale bar represent 100 μm.

days 0 and 14 with 5 μg IAV (VL group, $n = 3$), 25 μg IAV (VH group, $n = 3$), or sham vaccine (VC group, $n = 3$) followed with 10^6 $TCID_{50}$ per each SARS-CoV-2 challenge by intratracheal route for another 13 days after primary immunization. Blood samples or organs were collected at the indicated time points (Fig. 5A). All IAV-vaccinated RMs developed SARS-CoV-2 virion-specific antibodies or receptor binding domain (RBD) antibodies from day 7 and reached to a highest level at day 21 after vaccination (Fig. 5B, 5C). In contrast, in sham control monkeys we did not detect any SARS-CoV-2-specific antibody responses. The neutralizing antibody measured by

Fig. 3 Vaccinated mouse sera protect mice from SARS-CoV-2 infection. Vaccinated mouse sera were transferred to six to eight weeks old male HFH4-hACE2 mice. One day later, mice were challenged with 10^5 $TCID_{50}$ SARS-CoV-2 and monitored for 5 days. Experiment scheme was shown (**A**). Antibody level in HFH4-hACE2 mice was determined by virion-based IgG ELISA (**B**) and $PRNT_{50}$ (**C**). Days post infection (-1) represent the original vaccinated mouse sera antibody titer before transfer. No obvious difference was observed in mouse body weight change between each group (**D**). Lung viral load was determined by RT-qPCR (**E**). Error bars indicate the standard error. Statistical significance was measured by one-way ANOVA compared with the mock infected group. *$P < 0.05$. n.s. $P > 0.05$.
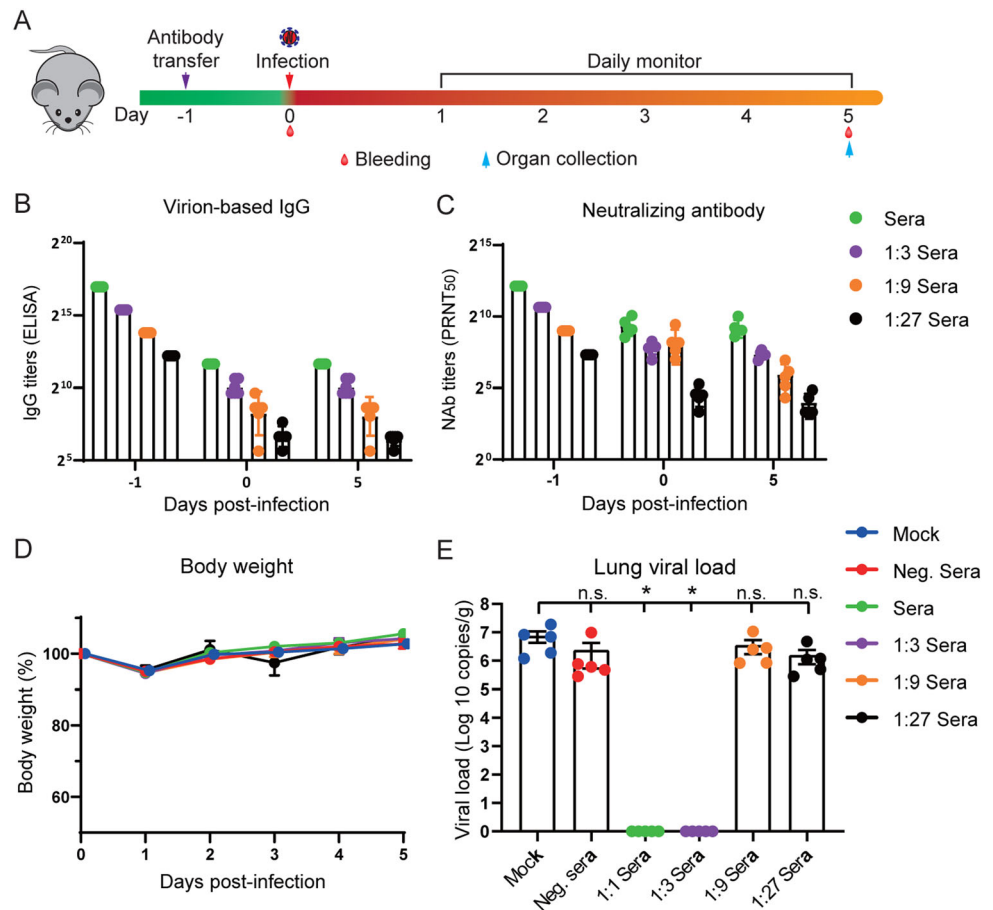
PRNT showed vaccinated animals generated significant and time-dependent increasing levels of neutralizing antibodies (Fig. 5D). The antibody titers were similar between high dose and low dose groups.

To examine the efficacy of the IAV, all the RMs were challenged by SARS-CoV-2 on day 23 after primary immunization. Upon infection, no obvious clinical signs were observed during the study course in all animals. The body weight (Fig. 6A) and body temperature (Fig. 6B) did not show any change for all RMs investigated in study course. However, vaccination does confer protection against SARS-CoV-2 infection to immunized RMs. The peak viral RNA load in oropharyngeal swab were between 3.2 to 9.6×10^5 copies/mL. In contrast, the RNA was undetectable in high dose group and showed deceased (less than 200 copies/mL) level in low dose group (Fig. 6C). The amount of viral RNA in respiratory tract was also investigated after necropsy. The data showed the viral RNA loads were ranging from 3.7×10^4 to 4.0×10^6 copies/g in trachea and bronchus samples on 4 day post challenge (d.p.c.). (Fig. 6C) and 2.0×10^4 copies/g in trachea on 9 d.p.c. (Fig. 6D). In contrast, no viral RNA loads could be detected from both VH and VL vaccinated groups.

Finally, the necropsy of lung in mock group showed large amount of fluid edema in the alveolar cavity, accompanied by fibrin exudation and hyaline membrane in early infection stage (4 d.p.c.). The alveolar walls were significantly thickened with a large of mononuclear and lymphocyte infiltration and fibroblast proliferation (Fig. 7A). As comparison, high-dose group only had mild pneumonia accompanied by focal or patchy lymphocyte infiltration and fibroblast proliferation, and low dose group showed mild-to-moderate interstitial pneumonia (Fig. 7B, 7C). Lastly, confocal microscopy analysis of lung tissues using specific antibodies (anti-SARS-CoV-2 N protein) indicated the positive viral N protein from VC groups on 4 d.p.c. while no positive signal could be detected from vaccinated groups (Supplementary Fig. S2).

Discussion

Among the different strategies of vaccine development, IAV shows its advantage by inducing immune responses against the complete viral structural proteins and its safety, but disadvantage of probably weak immune response due to the antigenicity losses during inactivation, thus need

Fig. 4 Pathological changes of passive transferred mice lung after challenge. Sera group and 1:3 dilution sera group show normal forms. Few exude of fibrin in some alveolar spaces in 1:3 dilution group was found (red arrow). In other four groups, lungs show similar pathological changes with mild peri-bronchial and peri-vascular infiltration (black arrow), alveolar exudation of fibrin (red arrow), and moderate alveolar wall thickening. Viral antigen was detected in lung bronchi and alveoli (red). Images were collected by using Pannoramic MIDI system. Black scale bar indicates 200 μm and white scale bar represents 100 μm.
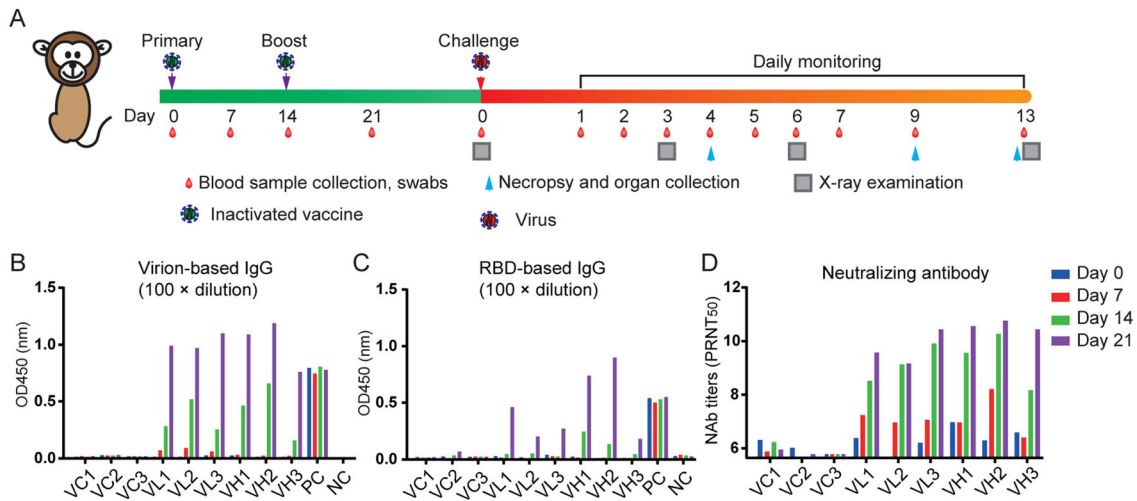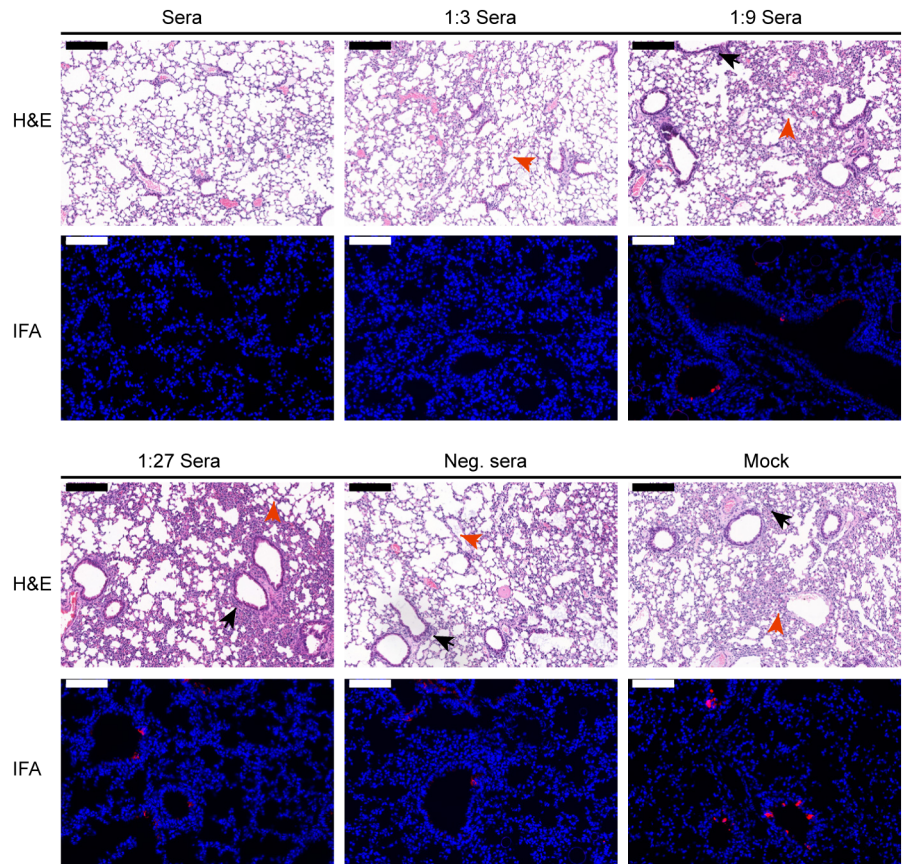

Fig. 5 Immunogenicity of the SARS-CoV-2 IAV in non-human primates. **A** Three rhesus macaques were immunized by the intramuscular route with 25 μg or 5 μg of IAV vaccine at weeks 0 and 2, respectively. Two were injected with an equal volume of the adjuvant. The animals were bled weekly to monitor the antibody response by ELISA or Plaque reduction neutralizing test (PRNT). SARS-CoV-2 RBD-specific ELISA titers (**B**), SARS-CoV-2 virion-based IgG titer (**C**), and neutralizing antibody (NAb) titers (**D**) in SARS-CoV-2 IAV immunized rhesus macaques. *RBD* receptor binding domain.
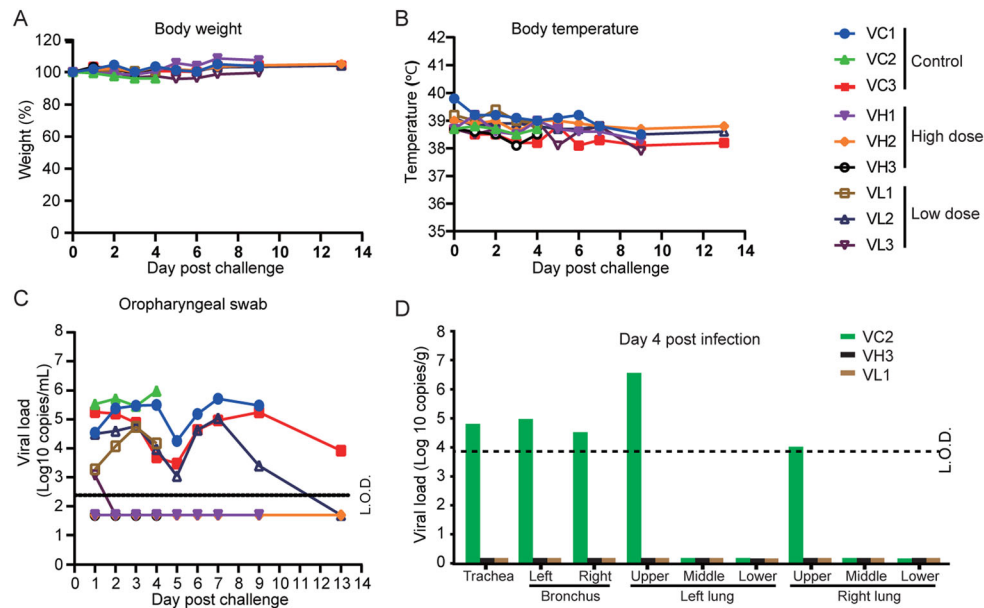
Fig. 6 Protective efficacy of the SARS-CoV-2 IAV. Nine immunized animals were challenged by 1×10^6 TCID$_{50}$ SARS-CoV-2 by intratracheal route on day 24 post of initial immunization. Disease parameters were measured including body weight, body temperature, and swabs. Viral loads in blood and swabs were monitored to evaluate viral replication kinetics in rhesus macaques. The viral RNA was extracted by Qiagen Viral RNA kit and followed by RT-qPCR to quantify viral RNA. **A** Body weight changes of rhesus macaques after infection with SARS-CoV-2. **B** Changes of the rectal temperature of RMs after infection with SARS-CoV-2. **C** Viral RNA load in oropharyngeal swab. **D** Viral RNA load in Viral loads in trachea, bronchus, right and left upper, middle, and lower lung lobes on day 4 (**B**), day 9 (**C**), and day 13 (**D**). *L.O.D.* limit of detection.
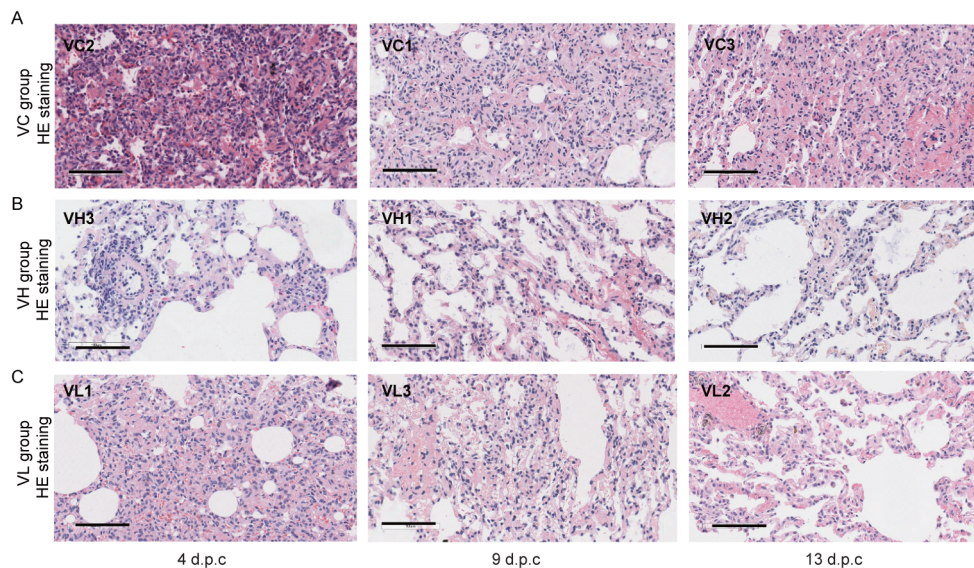
Fig. 7 Histopathological analysis of lung changes in rhesus macaques challenged with SARS-CoV-2. Eight rhesus macaques were challenged with SARS-CoV-2. Three animals were euthanized and necropsied on 4 d.p.c. and 9 d.p.c., respectively. And 2 animals were necropsied on 13 d.p.c. Histological analysis was performed on multiple shots. In addition, the inactivated vaccine development and process are generally mature in China, time-efficient and meet the demand of emergence usage. Here, we developed, tested the immunogenicity and protection tissues collected at 4 d.p.c., 9 d.p.c. and 13 d.p.c. HE (upper row) and Masson staining (lower row) of the lung tissues at 4 d.p.c., 9 d.p.c., and 13 d.p.c. for sham vaccine (VC) group (**A**), high dose (VH) group (**B**), and low dose (VL) group (**C**). Scale bar = 100 μm.

efficacy of SARS-CoV-2 IAV in two animal models, human ACE2 transgenic mice and rhesus macaques. Our data showed two-dose immunization could induce neutralizing antibody in rhesus macaques without significant

difference. Higher dose of IAV provided full protection against the SARS-CoV-2 infection by showing the undetectable viral RNA, antigen expression and histopathological changes in the challenge animal lung tissues. The low IAV dose group showed significantly decreased in viral RNA, antigen expression, and mild lung damage. These results demonstrate that our IAV is a promising vaccine to humans.

To further understand the role of neutralizing antibody in against SARS-CoV-2, the sera collected from immunized BALB/c mice also could provide full protection for HFH4-hACE2 mice from SARS-CoV-2 infection at neat or 1:3 dilution demonstrated by undetectable viral RNA in lung tissues. The higher dilutions of hyperimmune sera (1:9 and 1:27) did not show protection. The antibody in the animal body did not show obvious waning after 5 days of injection, indicating the potential emergency use of sera therapy from convalescent COVID-19 patients (Duan *et al.* 2020). Till 22nd January 2021, 64 and 73 candidate vaccines in clinical evaluation and preclinical evaluation, respectively (WHO 2020b). Based on different antigen selection, vaccine platform were divided into 8 catalogs, including inactivated, attenuated, non-replicating viral vector, replicating viral vector, protein subunit, mRNA, DNA, and viral-like particle (WHO 2020b). The first vaccine was for smallpox which was live attenuated vaccine in the eighteenth century (Stewart and Devlin 2006). However, acquisition of attenuated virus need serial passage *in vitro* or *in vivo*, which was inefficient (Plotkin 2014). In contrast, the killed whole organisms were used as inactivated vaccine at the nineteenth century in revolution based on cell culture *in vitro* (Plotkin and Plotkin 2011). Following the development of molecular technology, genetically engineered recombinant antigens were used for vaccine development, which was challenged by pre-existing immunity against the carrier vector (Zhang and Zhou 2016). Moreover, either DNA or RNA coding proteins or purified proteins also be innovated approach in recent years with easy produce and high yield, but also challenged with immunogenicity or delivery efficiency (Lundstrom 2015; Porter and Raviprakash 2017). Currently, five types of vaccine candidates including inactivated, non-replicating viral vector, protein subunit, DNA, and RNA were carried out on clinical phase 3 (WHO 2020b). Several mRNA vaccines have revealed their phase III clinical trials which shows high protection efficacy and highlights the future direction of vaccine development technique.

Starting from the 1960s, evaluations of vaccine candidates for infectious diseases such as dengue virus, zika virus, respiratory syncytial virus (RSV), and severe acute respiratory syndrome (SARS) have shown a paradoxical phenomenon: pre-existing antibody from vaccination in some animals or people could cause more severe disease when exposed to secondary infection which called antibody-dependent enhancement of infection (ADE) (Graham 2011; Bardina *et al.* 2017; Katzelnick *et al.* 2017; Luo *et al.* 2018). Neither weight loss nor fever were observed on the immunized mice or monkey in the study. We didn't observe any ADE in challenged mice with transferred hyperimmune sera of different dilutions. In conclusion, no evidence showed ADE from any vaccinated mice or macaques.

Our work has the limitation. We did not detect the role played by lymphocytes due to limited numbers of animals and techniques restrain. The vaccine can elicit the T cell response which has been demonstrated to play a crucial role in clearance of the acute viral infection. The cytokine storm which induced by excessive T cell response has been shown to correlate the severity of the COVID19 patients (Zheng *et al.* 2020). The previous study on inactivated vaccine showed the lymphocyte subset percent and key cytokines did not show notable changes after vaccination (Gao *et al.* 2020). The protection period that acts through T cell responses or B cell immune responses was needed to long time monitor.

Author Contributions YFY, ZJW, RDJ, XH, HJZ, YWZ, GG, YC, YP, MQL, YNZ, JM, JL, XXG, JG, CP, XRS, QL, KZ, LY, XW, BZ, WHW, and JW performed experiments and data analysis. PZ, XLY, SS, CS, ZMY, and ZLS designed the experiments and interpreted the results, CS, ZLS, XLY, and ZMY wrote the manuscript.

Compliance with Ethical Standards

Conflict of interest The authors declared that they have no conflict of interest.

Animal and Human Right All animal experiments were approved by the Institutional Animal Care and Use Committee (Ethics number: WIVA42202002) of Wuhan Institute of Virology, Chinese Academy of Sciences. The SARS-CoV-2 animal model experiments and protocols were also discussed explicitly and extensively with biosafety officers and facility managers at the Wuhan Institute of Virology. Non-human primate experiments were conducted within the animal biosafety level 4 (ABSL-4) facility and mice experiments were performed in animal biosafety level 3 (ABSL-3) laboratory in National Biosafety Laboratory (Wuhan), Chinese Academy of Sciences.

References

Bardina SV, Bunduc P, Tripathi S, Duehr J, Frere JJ, Brown JA, Nachbagauer R, Foster GA, Krysztof D, Tortorella D, Stramer SL, Garcia-Sastre A, Krammer F, Lim JK (2017) Enhancement of Zika virus pathogenesis by preexisting antiflavivirus immunity. Science 356:175–180

Baum A, Fulton BO, Wloga E, Copin R, Pascal KE, Russo V, Giordano S, Lanza K, Negron N, Ni M, Wei Y, Atwal GS, Murphy AJ, Stahl N, Yancopoulos GD, Kyratsous CA (2020) Antibody cocktail to SARS-CoV-2 spike protein prevents rapid mutational escape seen with individual antibodies. Science 369:1014–1018

Corbett KS, Edwards DK, Leist SR, Abiona OM, Boyoglu-Barnum S, Gillespie RA, Himansu S, Schafer A, Ziwawo CT, DiPiazza AT, Dinnon KH, Elbashir SM, Shaw CA, Woods A, Fritch EJ, Martinez DR, Bock KW, Minai M, Nagata BM, Hutchinson GB, Wu K, Henry C, Bahl K, Garcia-Dominguez D, Ma L, Renzi I, Kong WP, Schmidt SD, Wang L, Zhang Y, Phung E, Chang LA, Loomis RJ, Altaras NE, Narayanan E, Metkar M, Presnyak V, Liu C, Louder MK, Shi W, Leung K, Yang ES, West A, Gully KL, Stevens LJ, Wang N, Wrapp D, Doria-Rose NA, Stewart-Jones G, Bennett H, Alvarado GS, Nason MC, Ruckwardt TJ, McLellan JS, Denison MR, Chappell JD, Moore IN, Morabito KM, Mascola JR, Baric RS, Carfi A, Graham BS (2020a) SARS-CoV-2 mRNA vaccine design enabled by prototype pathogen preparedness. Nature 586:567–571

Corbett KS, Flynn B, Foulds KE, Francica JR, Boyoglu-Barnum S, Werner AP, Flach B, O'Connell S, Bock KW, Minai M, Nagata BM, Andersen H, Martinez DR, Noe AT, Douek N, Donaldson MM, Nji NN, Alvarado GS, Edwards DK, Flebbe DR, Lamb E, Doria-Rose NA, Lin BC, Louder MK, O'Dell S, Schmidt SD, Phung E, Chang LA, Yap C, Todd JM, Pessaint L, Van Ry A, Browne S, Greenhouse J, Putman-Taylor T, Strasbaugh A, Campbell TA, Cook A, Dodson A, Steingrebe K, Shi W, Zhang Y, Abiona OM, Wang L, Pegu A, Yang ES, Leung K, Zhou T, Teng IT, Widge A, Gordon I, Novik L, Gillespie RA, Loomis RJ, Moliva JI, Stewart-Jones G, Himansu S, Kong WP, Nason MC, Morabito KM, Ruckwardt TJ, Ledgerwood JE, Gaudinski MR, Kwong PD, Mascola JR, Carfi A, Lewis MG, Baric RS, McDermott A, Moore IN, Sullivan NJ, Roederer M, Seder RA, Graham BS (2020b) Evaluation of the mRNA-1273 Vaccine against SARS-CoV-2 in Nonhuman Primates. N Engl J Med 383:1544–1555

Coronaviridae Study Group of the International Committee on Taxonomy of V (2020) The species Severe acute respiratory syndrome-related coronavirus: classifying 2019-nCoV and naming it SARS-CoV-2. Nat Microbiol 5:536–544

Dagotto G, Yu J, Barouch DH (2020) Approaches and challenges in SARS-CoV-2 vaccine development. Cell Host Microbe 28:364–370

Duan K, Liu B, Li C, Zhang H, Yu T, Qu J, Zhou M, Chen L, Meng S, Hu Y, Peng C, Yuan M, Huang J, Wang Z, Yu J, Gao X, Wang D, Yu X, Li L, Zhang J, Wu X, Li B, Xu Y, Chen W, Peng Y, Hu Y, Lin L, Liu X, Huang S, Zhou Z, Zhang L, Wang Y, Zhang Z, Deng K, Xia Z, Gong Q, Zhang W, Zheng X, Liu Y, Yang H, Zhou D, Yu D, Hou J, Shi Z, Chen S, Chen Z, Zhang X, Yang X (2020) Effectiveness of convalescent plasma therapy in severe COVID-19 patients. Proc Natl Acad Sci USA 117:9490–9496

Gao Q, Bao L, Mao H, Wang L, Xu K, Yang M, Li Y, Zhu L, Wang N, Lv Z, Gao H, Ge X, Kan B, Hu Y, Liu J, Cai F, Jiang D, Yin Y, Qin C, Li J, Gong X, Lou X, Shi W, Wu D, Zhang H, Zhu L, Deng W, Li Y, Lu J, Li C, Wang X, Yin W, Zhang Y, Qin C (2020) Development of an inactivated vaccine candidate for SARS-CoV-2. Science 369:77–81

Graham BS (2011) Biological challenges and technological opportunities for respiratory syncytial virus vaccine development. Immunol Rev 239:149–166

Hoffmann M, Kleine-Weber H, Schroeder S, Kruger N, Herrler T, Erichsen S, Schiergens TS, Herrler G, Wu NH, Nitsche A, Muller MA, Drosten C, Pohlmann S (2020) SARS-CoV-2 cell entry depends on ACE2 and TMPRSS2 and Is blocked by a clinically proven protease inhibitor. Cell 181:271–280.e278

Jiang RD, Liu MQ, Chen Y, Shan C, Zhou YW, Shen XR, Li Q, Zhang L, Zhu Y, Si HR, Wang Q, Min J, Wang X, Zhang W, Li B, Zhang HJ, Baric RS, Zhou P, Yang XL, Shi ZL (2020) Pathogenesis of SARS-CoV-2 in transgenic mice expressing human angiotensin-converting enzyme 2. Cell 182:50–58.e58

Katzelnick LC, Gresh L, Halloran ME, Mercado JC, Kuan G, Gordon A, Balmaseda A, Harris E (2017) Antibody-dependent enhancement of severe dengue disease in humans. Science 358:929–932

Kissler SM, Tedijanto C, Goldstein E, Grad YH, Lipsitch M (2020) Projecting the transmission dynamics of SARS-CoV-2 through the postpandemic period. Science 368:860–868

Lundstrom K (2015) RNA-based drugs and vaccines. Expert Rev Vaccines 14:253–263

Luo F, Liao FL, Wang H, Tang HB, Yang ZQ, Hou W (2018) Evaluation of antibody-dependent enhancement of SARS-CoV infection in rhesus macaques immunized with an inactivated SARS-CoV vaccine. Virol Sin 33:201–204

Menachery VD, Yount BL Jr, Sims AC, Debbink K, Agnihothram SS, Gralinski LE, Graham RL, Scobey T, Plante JA, Royal SR, Swanstrom J, Sheahan TP, Pickles RJ, Corti D, Randell SH, Lanzavecchia A, Marasco WA, Baric RS (2016) SARS-like WIV1-CoV poised for human emergence. Proc Natl Acad Sci USA 113:3048–3053

Plotkin S (2014) History of vaccination. Proc Natl Acad Sci USA 111:12283–12287

Plotkin SA, Plotkin SL (2011) The development of vaccines: how the past led to the future. Nat Rev Microbiol 9:889–893

Porter KR, Raviprakash K (2017) DNA vaccine delivery and improved immunogenicity. Curr Issues Mol Biol 22:129–138

Shan C, Yao YF, Yang XL, Zhou YW, Gao G, Peng Y, Yang L, Hu X, Xiong J, Jiang RD, Zhang HJ, Gao XX, Peng C, Min J, Chen Y, Si HR, Wu J, Zhou P, Wang YY, Wei HP, Pang W, Hu ZF, Lv LB, Zheng YT, Shi ZL, Yuan ZM (2020) Infection with novel coronavirus (SARS-CoV-2) causes pneumonia in Rhesus macaques. Cell Res 30:670–677

Stewart AJ, Devlin PM (2006) The history of the smallpox vaccine. J Infect 52:329–334

Tostanoski LH, Wegmann F, Martinot AJ, Loos C, McMahan K, Mercado NB, Yu J, Chan CN, Bondoc S, Starke CE, Nekorchuk M, Busman-Sahay K, Piedra-Mora C, Wrijil LM, Ducat S, Custers J, Atyeo C, Fischinger S, Burke JS, Feldman J, Hauser BM, Caradonna TM, Bondzie EA, Dagotto G, Gebre MS, Jacob-Dolan C, Lin Z, Mahrokhian SH, Nampanya F, Nityanandam R, Pessaint L, Porto M, Ali V, Benetiene D, Tevi K, Andersen H, Lewis MG, Schmidt AG, Lauffenburger DA, Alter G, Estes JD, Schuitemaker H, Zahn R, Barouch DH (2020) Ad26 vaccine protects against SARS-CoV-2 severe clinical disease in hamsters. Nat Med 26:1694–1700

van Doremalen N, Lambe T, Spencer A, Belij-Rammerstorfer S, Purushotham JN, Port JR, Avanzato VA, Bushmaker T, Flaxman A, Ulaszewska M, Feldmann F, Allen ER, Sharpe H, Schulz J, Holbrook M, Okumura A, Meade-White K, Perez-Perez L, Edwards NJ, Wright D, Bissett C, Gilbride C, Williamson BN, Rosenke R, Long D, Ishwarbhai A, Kailath R, Rose L, Morris S, Powers C, Lovaglio J, Hanley PW, Scott D, Saturday G, de Wit E, Gilbert SC, Munster VJ (2020) ChAdOx1 nCoV-19 vaccine prevents SARS-CoV-2 pneumonia in rhesus macaques. Nature 586:578–582

Wang H, Zhang Y, Huang B, Deng W, Quan Y, Wang W, Xu W, Zhao Y, Li N, Zhang J, Liang H, Bao L, Xu Y, Ding L, Zhou W, Gao H, Liu J, Niu P, Zhao L, Zhen W, Fu H, Yu S, Zhang Z, Xu G, Li C, Lou Z, Xu M, Qin C, Wu G, Gao GF, Tan W, Yang X (2020) Development of an inactivated vaccine candidate, BBIBP-CorV, with potent protection against SARS-CoV-2. Cell 182:713–721.e719

Wang M, Cao R, Zhang L, Yang X, Liu J, Xu M, Shi Z, Hu Z, Zhong W, Xiao G (2020) Remdesivir and chloroquine effectively inhibit the recently emerged novel coronavirus (2019-nCoV) in vitro. Cell Res 30:269–271

Wang ZJ, Zhang HJ, Lu J, Xu KW, Peng C, Guo J, Gao XX, Wan X, Wang WH, Shan C, Zhang SC, Wu J, Yang AN, Zhu Y, Xiao A, Zhang L, Fu L, Si HR, Cai Q, Yang XL, You L, Zhou YP, Liu J, Pang DQ, Jin WP, Zhang XY, Meng SL, Sun YX, Desselberger U, Wang JZ, Li XG, Duan K, Li CG, Xu M, Shi ZL, Yuan ZM, Yang XM, Shen S (2020) Low toxicity and high immunogenicity of an inactivated vaccine candidate against COVID-19 in different animal models. Emerg Microbes Infect 9:2606–2618

WHO (2020a) Coronavirus disease (COVID-2019) situation reports. https://www.who.int/emergencies/diseases/novel-coronavirus-2019/situation-reports/

WHO (2020b) Draft landscape of COVID-19 candidate vaccines. https://www.who.int/publications/m/item/draft-landscape-of-covid-19-candidate-vaccines

Wu S, Zhong G, Zhang J, Shuai L, Zhang Z, Wen Z, Wang B, Zhao Z, Song X, Chen Y, Liu R, Fu L, Zhang J, Guo Q, Wang C, Yang Y, Fang T, Lv P, Wang J, Xu J, Li J, Yu C, Hou L, Bu Z, Chen W (2020) A single dose of an adenovirus-vectored vaccine provides protection against SARS-CoV-2 challenge. Nat Commun 11:4081

Xia S, Duan K, Zhang Y, Zhao D, Zhang H, Xie Z, Li X, Peng C, Zhang Y, Zhang W, Yang Y, Chen W, Gao X, You W, Wang X, Wang Z, Shi Z, Wang Y, Yang X, Zhang L, Huang L, Wang Q, Lu J, Yang Y, Guo J, Zhou W, Wan X, Wu C, Wang W, Huang S, Du J, Meng Z, Pan A, Yuan Z, Shen S, Guo W, Yang X (2020) Effect of an inactivated vaccine against SARS-CoV-2 on safety and immunogenicity outcomes: interim analysis of 2 randomized clinical trials. JAMA 324:951–960

Yang J, Wang W, Chen Z, Lu S, Yang F, Bi Z, Bao L, Mo F, Li X, Huang Y, Hong W, Yang Y, Zhao Y, Ye F, Lin S, Deng W, Chen H, Lei H, Zhang Z, Luo M, Gao H, Zheng Y, Gong Y, Jiang X, Xu Y, Lv Q, Li D, Wang M, Li F, Wang S, Wang G, Yu P, Qu Y, Yang L, Deng H, Tong A, Li J, Wang Z, Yang J, Shen G, Zhao Z, Li Y, Luo J, Liu H, Yu W, Yang M, Xu J, Wang J, Li H, Wang H, Kuang D, Lin P, Hu Z, Guo W, Cheng W, He Y, Song X, Chen C, Xue Z, Yao S, Chen L, Ma X, Chen S, Gou M, Huang W, Wang Y, Fan C, Tian Z, Shi M, Wang FS, Dai L, Wu M, Li G, Wang G, Peng Y, Qian Z, Huang C, Lau JY, Yang Z, Wei Y, Cen X, Peng X, Qin C, Zhang K, Lu G, Wei X (2020) A vaccine targeting the RBD of the S protein of SARS-CoV-2 induces protective immunity. Nature 586:572–577

Yu J, Tostanoski LH, Peter L, Mercado NB, McMahan K, Mahrokhian SH, Nkolola JP, Liu J, Li Z, Chandrashekar A, Martinez DR, Loos C, Atyeo C, Fischinger S, Burke JS, Slein MD, Chen Y, Zuiani A, Lelis FJN, Travers M, Habibi S, Pessaint L, Van Ry A, Blade K, Brown R, Cook A, Finneyfrock B, Dodson A, Teow E, Velasco J, Zahn R, Wegmann F, Bondzie EA, Dagotto G, Gebre MS, He X, Jacob-Dolan C, Kirilova M, Kordana N, Lin Z, Maxfield LF, Nampanya F, Nityanandam R, Ventura JD, Wan H, Cai Y, Chen B, Schmidt AG, Wesemann DR, Baric RS, Alter G, Andersen H, Lewis MG, Barouch DH (2020) DNA vaccine protection against SARS-CoV-2 in rhesus macaques. Science 369:806–811

Zhang C, Zhou DM (2016) Adenoviral vector-based strategies against infectious disease and cancer. Human Vaccin Immunother 12:2064–2074

Zheng HY, Zhang M, Yang CX, Zhang N, Wang XC, Yang XP, Dong XQ, Zheng YT (2020) Elevated exhaustion levels and reduced functional diversity of T cells in peripheral blood may predict severe progression in COVID-19 patients. Cell Mol Immunol 17:541–543

Zhou P, Yang XL, Wang XG, Hu B, Zhang L, Zhang W, Si HR, Zhu Y, Li B, Huang CL, Chen HD, Chen J, Luo Y, Guo H, Jiang RD, Liu MQ, Chen Y, Shen XR, Wang X, Zheng XS, Zhao K, Chen QJ, Deng F, Liu LL, Yan B, Zhan FX, Wang YY, Xiao GF, Shi ZL (2020) A pneumonia outbreak associated with a new coronavirus of probable bat origin. Nature 579:270–273